

# Euro-Atlantic circulation types and modes of variability in winter in ERA-40 and NCEP reanalyses

M.J. Casado<sup>1</sup>, M.A. Pastor<sup>1</sup>, F.J. Doblas-Reyes<sup>2</sup>

Research Department

<sup>1</sup> Instituto Nacional de Meteorología, Madrid, Spain  
<sup>2</sup> ECMWF

Submitted to Theoretical and Applied Climatology

January 2008

This paper has not been published and should be regarded as an Internal Report from ECMWF.  
Permission to quote from it should be obtained from the ECMWF.



European Centre for Medium-Range Weather Forecasts  
Europäisches Zentrum für mittelfristige Wettervorhersage  
Centre européen pour les prévisions météorologiques à moyen

**Series: ECMWF Technical Memoranda**

A full list of ECMWF Publications can be found on our web site under:  
<http://www.ecmwf.int/publications/>

Contact: [library@ecmwf.int](mailto:library@ecmwf.int)

**© Copyright 2008**

European Centre for Medium Range Weather Forecasts  
Shinfield Park, Reading, Berkshire RG2 9AX, England

Literary and scientific copyrights belong to ECMWF and are reserved in all countries. This publication is not to be reprinted or translated in whole or in part without the written permission of the Director. Appropriate non-commercial use will normally be granted under the condition that reference is made to ECMWF.

The information within this publication is given in good faith and considered to be true, but ECMWF accepts no liability for error, omission and for loss or damage arising from its use.

## Abstract

Extra-tropical atmospheric circulation variability is addressed in this study using two complementary approaches: circulation types and modes of variability. Principal component analysis (PCA) in T- and S-modes has been used to estimate the features. An objective synoptic classification of Euro-Atlantic atmospheric circulation is described. Eight circulation types have been identified and described in terms of their spatial features, mean frequency and lifetime, transitions and trends. The most persistent type is connected with the presence of a ridge over the British Isles and Iceland, while the less persistent type is related to a tilted ridge west of the continent. Increases in the persistence of some circulation types such as the Scandinavian and the Euro-Atlantic blockings and a ridge with axis over Western Europe have been found in the 1990s. Data from two independent re-analyses are used to test the robustness of the results. The main differences between the two datasets have been found in the distribution of events as a function of their duration. In a second step, the main modes of variability over the Euro-Atlantic area have been identified using daily data. An analysis of the relationship between these modes and the circulation types suggests that specific circulation types shift the phases of certain modes of variability.

## 1. Introduction

The large-scale circulation of the atmosphere in the extra-tropical regions can be described by the alternation of circulation types (CTs), also known as weather regimes. Changes in the properties of the CTs are an important topic for the characterization of the variability of both observed climate and climate simulations. For instance, the identification of CTs associated with climate extreme events is expected to become more and more important to determine the possible changes of climate extremes induced by the enhanced greenhouse effect (SánchezGómez and Terray, 2005).

CTs have been usually characterized by different subjective and objective classification methods. The subjective methods (Lamb, 1950) have been based on visual interpretation of the surface synoptic maps and show serious drawbacks like the dependence of the assignment of a map to a particular pattern. In contrast, objective methods try to classify a set of maps using statistical techniques. Huth (1996) distinguished among four types of objective methods using correlations (Lund, 1963) or sums of squares (Kirchhofer, 1973) as cost function, cluster analysis (Key and Crane, 1986; Kidson, 1994) and finally analysis based on eigentechniques (Richman, 1986). He found, in agreement with Jiang et al. (2006), that no method was indisputably superior. Compagnucci and Salles (1997) used principal component analysis (PCA) to obtain CTs of daily July pressure fields over South America that were in good agreement with the types empirically identified by weather forecasters, enhancing the relevance of the human component. Richman (1986) employed different PCA-based techniques (in particular, PCA followed by either orthogonal or oblique rotation of the eigenvectors) to support the use of rotated solutions. Bartzokas and Metaxas (1996) also employed rotated PCA to avoid some drawbacks of the PCA. In spite of the benefits of rotation in PCA-based classifications, Compagnucci and Salles (1997) showed that sound classifications could also be obtained without rotation. Kysely and Huth (2006) advocated, for the first time, the use of both objective and subjective classifications as complementary methods and, in fact, a growing body of opinion seems to support this point of view. In summary, experience suggests that it is up to the scientist to select, based mainly on experience and collaboration with synopticians, the most appropriate method according to the target of the study.

In the past, a large number of studies focused mainly on changes in frequencies of the Euro-Atlantic CTs: Slonosky et al. (2000) applying an EOF analysis revealed that the most important circulation regimes are the

zonal and blocking/cyclonic flows in the eastern Atlantic and western Europe; Plaut and Simmonet (2001) found four 500-hPa regimes, Atlantic Ridge, Blocking, Greenland anticyclone, Greenwich Trough and Zonal with interannual variability. Comparatively, few studies have focused on changes in the mean lifetime of the CTs. Recently, Kyselý and Domonkos (2006, KD henceforth) analyzed the Hess-Brezowsky (HB) classification (1952) of Grosswetterlagen over Europe since 1881 and noticed a sharp increase in the mean lifetime of the circulation patterns from the 1970s to the late 1980s for all seasons. Werner et al. (2000) were the first ones to identify the decade 1981-1990 as the onset of a shift in the Euro-Atlantic CTs on the basis of a change in mean lifetime of the west CT from the HB catalogue. Kyselý and Huth (2006) also found an increase around 1990 in the mean lifetime of atmospheric circulation in winter for all groups of their objectively defined CTs, although this increase was not as noticeable as for the HB CTs. This recent enhanced persistence of the atmospheric circulation may have also supported the more frequent occurrence of temperature and other climatic extremes in Europe recently and seems to be consistent with some climate change projections. It must also be taken into account that atmospheric blocking is a dynamical feature with major consequences for European climate (Doblas-Reyes et al., 2002) and it is likely that the mean duration of certain circulation types could be influenced by the extraordinary persistence of blocking events.

Another approach to the study of the atmospheric circulation variability consists in the use of modes of variability or teleconnection patterns. These large-scale atmospheric patterns have been employed in many studies (Blackmon et al. 1984; Hsu and Wallace 1985; Barnston and Livezey 1987; Thompson and Wallace 1998), but there are not many addressing the connection between CTs and modes of variability on a daily basis. This study tries to look at relationships between them.

The aim of this paper is twofold. Firstly, to provide an objective synoptic-climatic classification of wintertime mid-tropospheric atmospheric circulation over the Euro-Atlantic domain, focusing on the robustness of the estimates of frequency, mean lifetime, transitions and trends using two different re-analyses. As a second objective, the paper analyses the relationship between the CTs obtained with the major modes of variability in the Euro-Atlantic region. The text is organized as follows. The description of the datasets can be found in Section 2 and the methodology is presented in Section 3. In Section 4, the frequency, mean lifetime, transitions and trends of the CTs identified are summarized, while Section 5 addresses the issue of the relationship between CTs and modes of variability. The main conclusions are drawn in Section 6.

## 2. Data

Two gridded (on a  $2.5^\circ \times 2.5^\circ$  latitude-longitude regular grid) daily 500-hPa geopotential height (Z500) quasi-independent re-analysis over the period 1962-2002 have been used: the latest re-analysis produced at the European Centre for Medium-Range Weather Forecasts (ERA-40 henceforth; Uppala et al., 2005) and the one available from the National Centers for Environmental Prediction (NCEP henceforth; Kalnay et al., 1996). The study has been carried out for the extended winter season December-to-March (DJFM, 121 days), the season with the largest variability over the extratropical Northern Hemisphere. The spatial domain considered is the Euro-Atlantic region, which extends from  $25^\circ$  N to  $70^\circ$  N and from  $45^\circ$ W to  $50^\circ$ E. This makes a total of 741 grid points (39 in longitude and 19 in latitude), and 4,961 days (121 days times 41 winters). In the following, each winter is referred to with the year of the month of January included in the season.

### 3. Methodology

The classification starts with a PCA, i.e.  $\mathbf{Z}=\mathbf{F}\mathbf{A}^T$ , where  $\mathbf{Z}$  is the input data matrix ( $N \times n$ ),  $\mathbf{F}$  is the principal component (PC) score matrix ( $N \times n$ ) and  $\mathbf{A}$  is the loading matrix ( $n \times n$ ),  $N$  being the number of observations and  $n$  the number of variables. The loadings, or empirical orthogonal functions (EOFs), are eigenvectors of a similarity matrix (covariance or correlation)  $\mathbf{S}=(N-1)^{-1}\mathbf{Z}^T\mathbf{Z}$ , scaled by the square root of the corresponding eigenvalues. The eigenvalues are the variance explained by each PC. Typically, many of the  $n$  dimensions of  $\mathbf{A}$  represent mostly noise and are discarded based on some eigenvalue selection rules. The retained  $r$  eigenvectors produce a reduced matrix so  $\mathbf{F}'$  ( $N \times r$ ) while  $\mathbf{A}$  becomes  $\mathbf{A}'$  ( $n \times r$ ) (Richman, 1986; 1999).

The input data matrix  $\mathbf{Z}$  can be specified in several ways, depending on which magnitudes are treated as variables and observations. Two possibilities are commonly used for a meteorological field, either the grid point values are referred to as variables and the time steps as observations, which is known as S-mode, or the time steps as variables and the grid points as observations in the so-called T-mode. While the S-mode isolates groups of grid points varying similarly in time, the T-mode isolates groups of time steps with similar spatial patterns. In this study we have applied both approaches, the T-mode to obtain the CTs and the S-mode to estimate the modes of variability. In the first case, we constructed  $\mathbf{Z}$  from the winter unfiltered Z500 daily anomalies and carried out the PCA using a covariance matrix with 4,961 times 4,961 elements. The use of the correlation matrix was discarded because the CTs obtained were less discriminated, while the covariance matrix is justified by the quasi-stationary behaviour of the Z500 standard deviation on a day by day basis for a single grid point, as shown in Figure 1. In the case of the S-mode analysis, the PCA was carried out on a covariance matrix with 741 times 741 elements, with each element weighted by the normalized cosine of the latitude of the grid point.

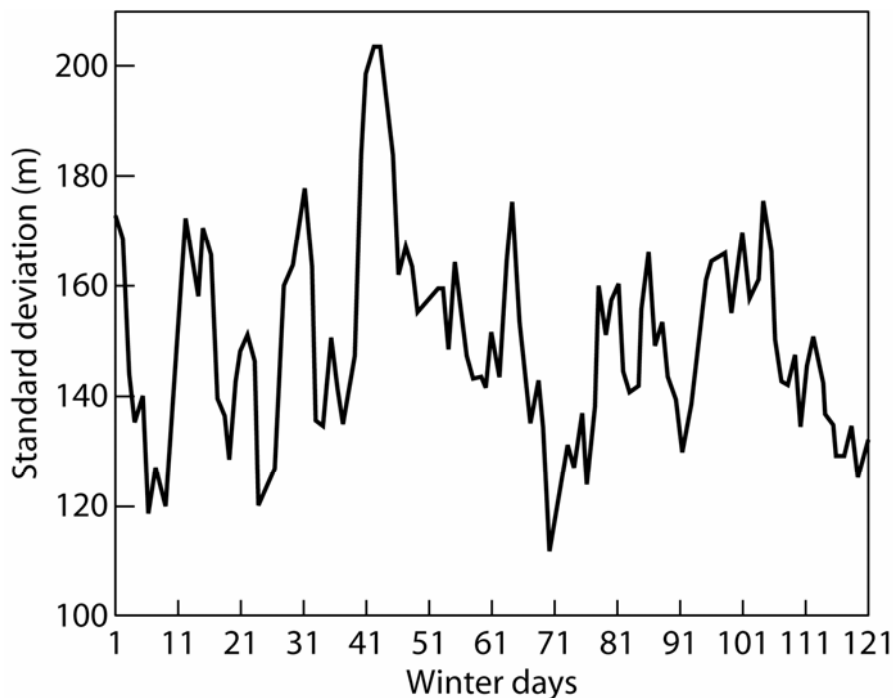


Figure 1: Interannual standard deviation on a day by day basis over winter (from the 1<sup>st</sup> of December to the 31<sup>st</sup> of March) at a single grid point for ERA-40.

A shortcoming of the PCA is that the eigenvectors are mathematical constructions constrained by their mutual orthogonality and the maximization of variance over the entire analysis domain so that no link to physical entities is guaranteed. The use of PCA can force the analysis to merge or blend patterns that would be otherwise independent (Richman, 1986). An alternative to reduce the effect of this drawback consists in rotating the empirical orthogonal functions and the corresponding PCs. The varimax orthogonal rotation (Richman, 1986), which is the most widely used rotation technique with statistically stable patterns (Cheng and Dunkerton, 1995), has been used. Following von Storch and Zwiers (1999), the PCs were previously renormalized to have unit variance to keep them uncorrelated after rotation. The classification was carried out for both rotated and unrotated solutions, obtaining very similar CTs in both cases. The rotated solutions were retained because they provide more discrimination in the frequency of occurrence of the CTs. For instance, while the frequency of occurrence for the unrotated CTs ranges between 11.1 % and 13.6 %, for the rotated solutions they are found within the range 10.7 % and 14.3 %.

To determine the number  $r$  of PCs, a log-eigenvalue versus PC number (LEV) diagram was used (Figure 2a). This diagram shows the log-eigenvalues for each PC in decreasing order. The number  $r$  is chosen as the number of log-eigenvalues which lie above the leftward extrapolation of the straight-line portion on its right hand side (Wilks, 2006). Figure 2a suggests a cut at the fourth eigenvalue. This choice is not unambiguous, so we have studied the impact of  $r$  examining the CTs obtained for different values of  $r$ . Tests were carried out with  $r$  ranging from 4 to 9. The CTs obtained for  $r=4$  are very similar to the first eight CTs obtained for all the other values of  $r$ : the mean lifetime ranges from 2.1 to 3.9 days. By contrast, the mean lifetime for the ninth and above CTs obtained for  $r>4$  have a much lower lifetime, ranging between 1.1 to 1.8 days. Hence, only four PCs were retained for rotation. The cumulative percentage of variance explained by the four leading PCs is 65%. Similar results were found for both ERA-40 and NCEP. As the loadings may be either positive or negative, twice as many CTs as PCs can be obtained. In the case dealt with here, eight CTs are provided by the four rotated PCs. We have considered the CTs as the composites of the maps that are assigned to each CT.

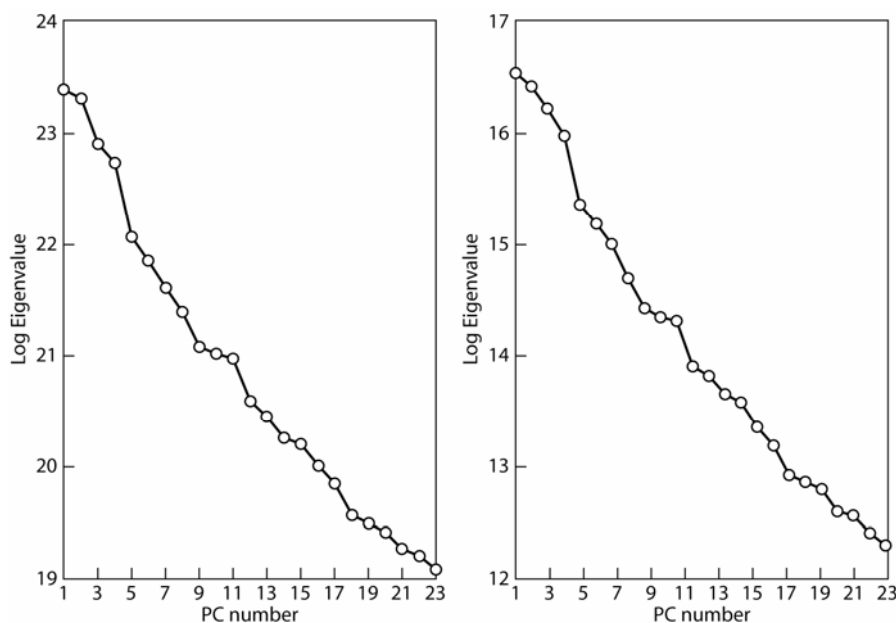


Figure 2: Log-eigenvalue versus principal component rank of the T-mode (left) and S-mode (right) principal component analysis of the ERA-40 500 hPa geopotential height dataset.

The T-mode PCA approach results in score patterns describing frequently occurring maps. The loadings indicate how much a pattern explains a specific map, allowing the identification of time periods when the maps are similar in a statistical sense to specific patterns (Huth, 1997). The degree of similarity of a circulation pattern to a CT is expressed by the corresponding loading, the higher the loading (in an absolute sense) the greater the similarity. This allows the classification of the daily circulation patterns depending on the PC with the highest loading (Jiang, 2006). A shortcoming of this simple approach is the uncertainty of how classifying maps with high loadings on more than one PC (neighbour loadings). An option to alleviate this problem consists in classifying only those days for which the loading exceeds a threshold, which implies that not all maps can be classified. To assess the impact of considering a threshold for the loading beyond which a map is classified in a CT, or neighbouring problem, a histogram (not shown) was constructed with the frequencies of the differences (in absolute value) between the two highest loadings for different thresholds from 0.0 (no threshold) to 0.9, at 0.1 intervals. The histogram suggests that the frequency of maps with neighbour loadings diminishes as the threshold increases. However, for small differences the discrimination when the threshold increases is small. For instance, for differences less than 0.2, the frequency of neighbour loadings decreases only from 25% (no threshold) to 18 % (threshold of 0.9). It can be concluded that the use of a threshold does not solve properly the problem of neighbour loadings. Nevertheless, we have analyzed the impact of using both a threshold classifying only the days with the highest loading being above 0.7 (which implies that 243 days are not classified) and the same threshold plus the constraint of not classifying those days in which the difference between the two highest loadings does not exceed 0.3 (243+1549 not classified days). The corresponding eight CTs obtained in these two classifications are very similar to those obtained without any threshold, suggesting a high robustness for this methodology. As the selection of a threshold does not significantly change the classification and introduces additional subjectivity, we decided not to use any threshold and allocate all the days to some CT.

## 4. Circulation types

### 4.1 General description

The Z500 CTs for ERA-40 are depicted in Figure 3, along with the total number of days classified in each of them. The CTs shown are not exactly the same as the score patterns obtained in the T-mode analysis as they have been obtained as the composites of the maps classified in each CT. This explains the lack of symmetry between the positive and negative pairs. Identical CTs are found for NCEP, the correlation between the corresponding CT patterns in both re-analyses being of the order of 0.99. A brief description of the CTs can be found in Table 1.

Circulation Types	Description
CT 1+	Ridge with axis from the Iberian Peninsula to Scandinavia
CT 1-	Atlantic ridge with axis south of Iceland
CT 2+	Scandinavian blocking
CT 2-	Atlantic ridge as an extension of the Azores anticyclone
CT 3+	Ridge tilted from the Southeast Atlantic to the central Europe
CT 3-	Ridge over the Iceland with zonal flow over central and southern Europe
CT 4+	Euro-Atlantic blocking with centre over the British Isles
CT 4-	Zonal flow

*Table 1: Circulation types obtained with four leading principal components.*

There are common features of this classification with other classifications performed over the European region. Four of the CTs obtained closely resemble the four NCEP Z500 regimes identified by Yiou and Nogaj (2004) using the clustering technique described in Michelangeli et al. (1995). Their regime “positive NAO” compares with CT1+, the “negative NAO” with the CT3-, the “Scandinavian blocking” with CT2+, and the “Atlantic ridge” with CT2-. However, Yiou and Nogaj (2004) only considered four weather regimes, which makes impossible to match the eight CTs with their classification. Our results also compared well with the weather types identified by Huth (1996, 2000) and with the HB-based objective classification published by James (2007). For instance the Cyclonic Westerly, Cyclonic Northerly, Icelandic High and Anticyclonic North Westerly are similar to the CTs 4-, 2-, 3- and 2+, respectively.

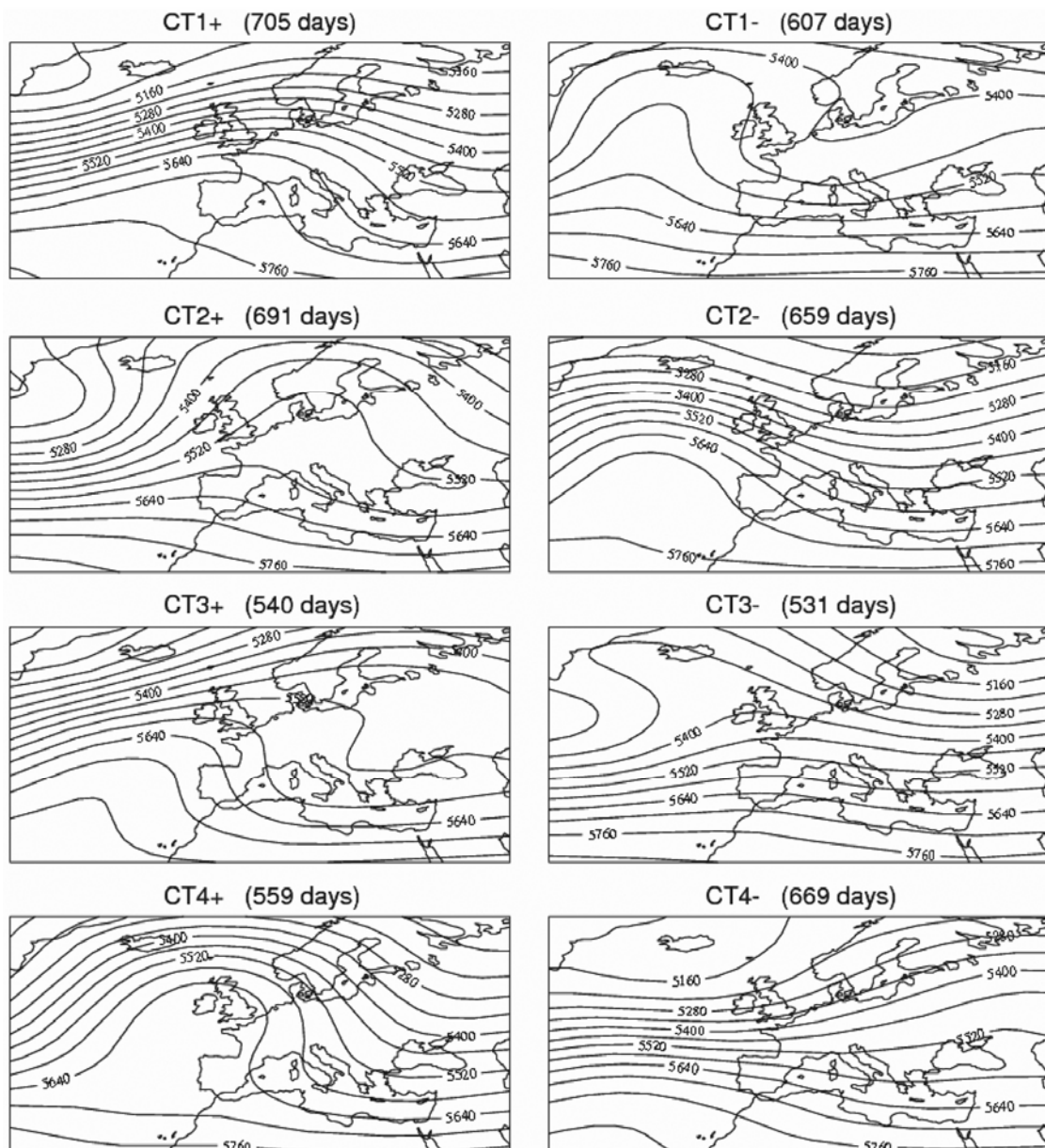


Figure 3: Circulation types for the classification of the ERA-40 500 hPa geopotential height over the period 1962-2002 using the four leading principal components with rotation. The circulation types have been obtained as the composites of the maps classified in each of them, which are indicated on top of each panel. Contours in metres.

## 4.2 Frequency and duration

The frequency of occurrence of the CTs is shown in Table 2. For both ERA-40 and NCEP, the most frequent CT turns out to be CT1+. As mentioned in the previous subsection, this CT resembles the zonal flow regime identified in Yiou and Nogaj (2004), which has strong links to the positive phase of the North Atlantic Oscillation (NAO). The least frequent types are CT3+ and CT3-.

Circulation Types	ERA-40		NCEP	
	Mean frequency	Mean lifetime	Mean Frequency	Mean lifetime
CT 1+	14.2	3.2	14.3	3.2
CT 1-	12.2	3.4	12.4	3.3
CT 2+	13.9	3.3	13.9	3.2
CT 2-	13.3	2.8	13.2	2.8
CT 3+	10.9	2.3	10.6	2.3
CT 3-	10.7	3.7	10.7	3.6
CT 4+	11.3	3.1	11.1	2.9
CT 4-	13.5	3.2	13.8	3.2

*Table 2: Relative frequency of occurrence (%) and mean duration (days) of the circulation types obtained for the ERA-40 and NCEP re-analyses with a classification using the four leading principal components.*

The interannual variability of the CT frequency is high, as shown in Figure 4, with some CTs happening more than one third of the days in a winter, while other CTs do not happen at all. There is also some decadal variability. For instance, an increase in the frequency of CT1+ is evidenced from the 1970s to the early 1990s. A Mann-Kendall test does not indicate statistically significant trends at the 5% significance level.

An interesting characteristic of the extra-tropical circulation is its persistence. Persistence can be expressed in terms of the mean duration of the events, or mean lifetime. An event is defined as an uninterrupted sequence of maps classified in the same CT, preceded and succeeded by maps classified in another CT. Table 3 shows the mean lifetime, which is around 3 days, the percentage of time spent in the events lasting at least four days, which is relatively high (~60%) and the number of one-day or transition events (~10% of the days) as defined in Huth (1997). Histograms of the number of events as a function of their duration are shown in Figure 5 for ERA-40 (blue) and for NCEP (red). The duration of the events has been proven to closely fit a geometric distribution. This can be compared with the mean lifetime of each CT in Table 2 to see that the CTs with the shortest mean lifetime have a larger proportion of short events. The longer-lived CTs are connected with Atlantic ridges (CT1- and CT3-), while the shortest (CT3+) correspond to a ridge over Western Europe. As CT2+ and CT4+ appear as blocking situations, it is likely that the mean lifetime of these CTs might be influenced by the extraordinary persistence of blocking events. While there is a substantial amount of events lasting longer than four days, a large fraction of the maps is classified as 1-day events. The differences between both re-analyses illustrated in Table 3 and Figure 5 are rather surprising. The number of 1-day events is larger for NCEP (568 days) than for ERA-40 (537 days). This is due to large differences in transition events in CTs 2+, 2- and 4+, which are more frequent in NCEP than in ERA-40. These differences, along with smaller ones in longer-lived events (Figure 5), suggest that some of the characteristics of the CTs are subject to observational uncertainty. This lack of robustness leads to careful interpretation of the details of circulation classifications and invites to use as many data sources as possible in this type of studies. Similar results are found for both NCEP and ERA-40.

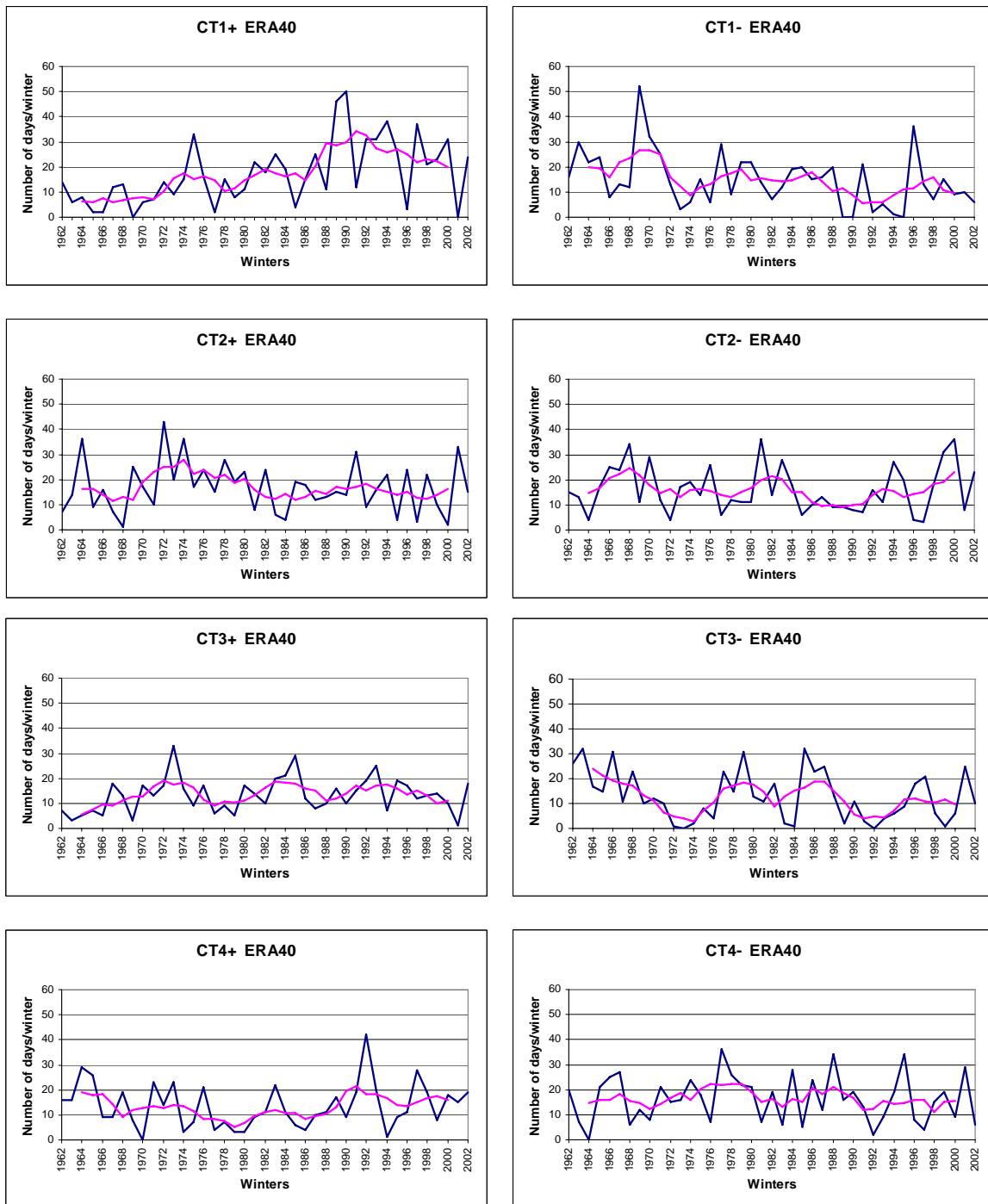


Figure 4: Number of days classified for each circulation type per winter for ERA-40 over the period 1962-2002. The pink line corresponds to a 5-year moving average.

	ERA-40	NCEP
M	3.1	3.0
>=4	60.7	60.0
1	537	568

Table 3: Mean lifetime (M), percentage of maps classified as events lasting at least four days or more (>=4) and number of 1-day events for the ERA-40 and NCEP re-analyses with a classification using the four leading principal components.

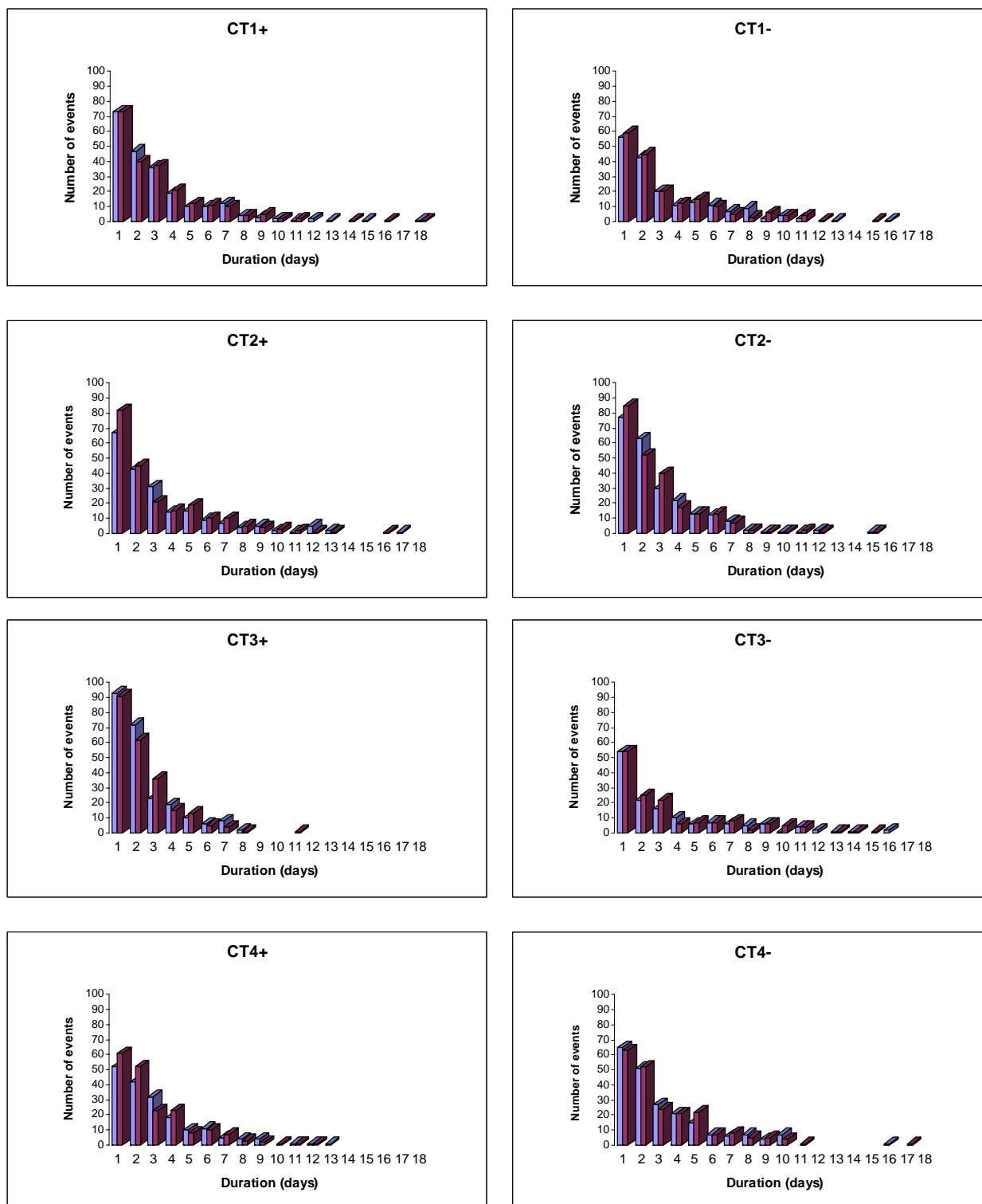


Figure 5: Number of events in each circulation type as a function of the duration in days for the ERA-40 (blue) and NCEP (red) classifications over the period 1962-2002.

The interannual variation of the mean lifetime is displayed in Figure 6. In general, as for the mean frequency, there is a substantial interannual variability, but the decadal variations illustrated by the moving average are of a smaller amplitude. A comparison of Figures 4 and 6 suggests that there is some correlation between the

mean frequency and the mean lifetime for certain CTs, as for example CT2-, 3- and 4-. These results are very similar for both re-analyses, although until 1975 ERA-40 exhibits a slightly larger mean lifetime (not shown), which points at an increased uncertainty in the results for the pre-satellite era.

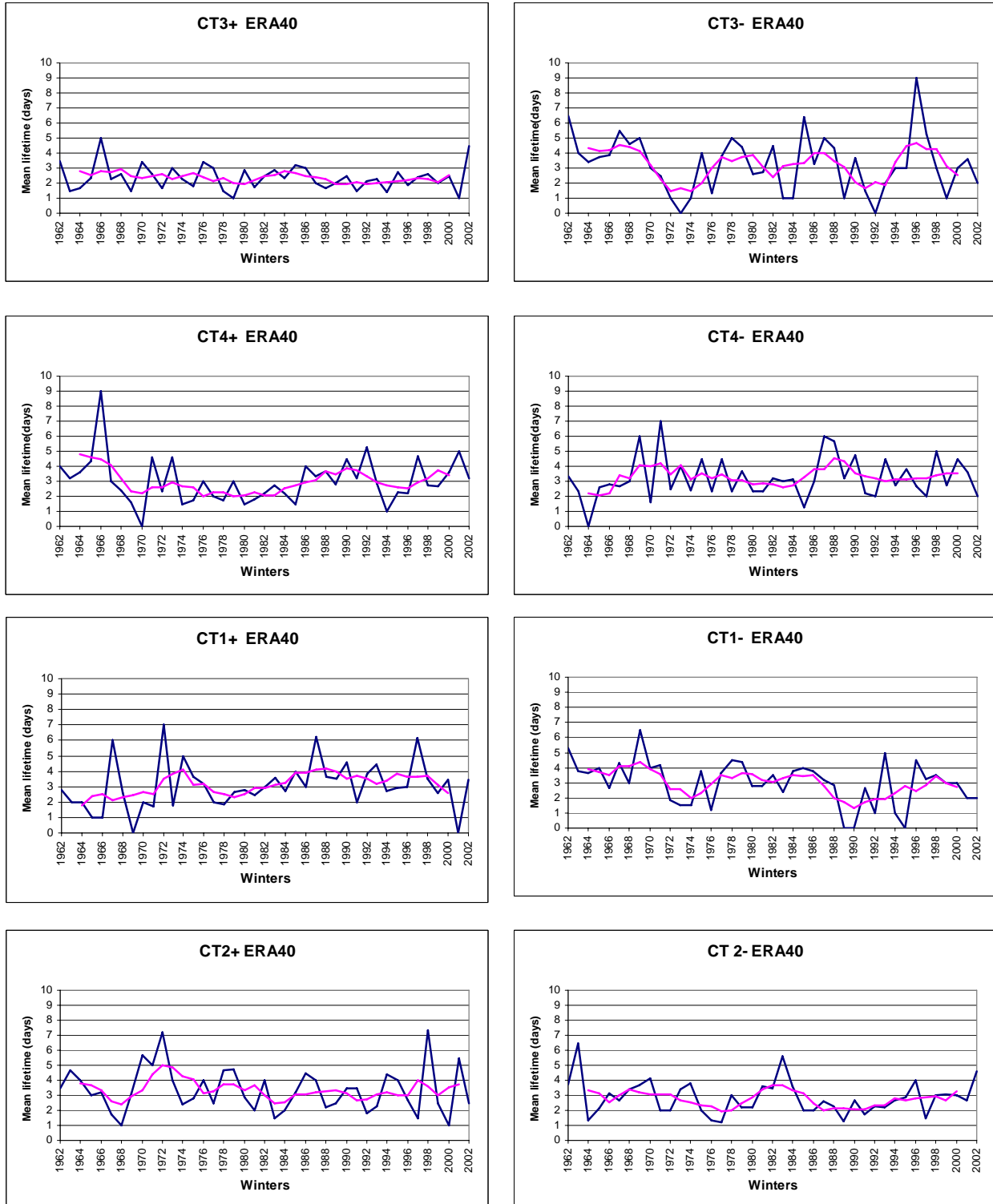


Figure 6: Mean lifetime of the circulation types per winter for the ERA-40 classification over the period 1962-2002. The pink line corresponds to a 5-year moving average.

### 4.3 Transitions between circulation types

SánchezGómez and Terray (2005) suggested that the development of a transition may be a process purely internal to the atmospheric dynamics connected to phase changes of intraseasonal atmospheric waves. James (2007) has recently pointed out that if any particular Grosswetterlagen is followed by a small number of specific types, a measure of medium-range predictability could be obtained.

The transitions between a specific CT and the other CTs are described in Table 4 for the ERA-40 classification. The transitions are expressed as the ratio between the number of changes from a CT to another one to the total number of changes from that CT. There are clearly preferred paths of change. The most probable transitions occur from CT1+ to CT2- and from CT2+ to CT3+, which in both cases consist in a regression of ridges that might eventually lead to a blocking event. The least probable transition is found from CT1- to CT4-, i.e., it is very unlikely that a zonal flow configuration develops into an Atlantic ridge in one day. In contrast, the zonal flow CT4- tends to be followed by the Scandinavian blocking (CT2+) or some sort of Atlantic ridge (CTs 1- and 2-). The Atlantic ridges (CTs 2- and 3+) tend to be followed by either the CT1+, which is linked to the positive phase of the NAO as shown in the following section, or lead to some sort of European blocking (CTs 2+ and 4+). These preferred paths of transition could be used to enhance the predictability of medium-range and extended predictions, although they could prove more useful to understand missed transitions in specific dynamical weather forecasts or climate simulations. Similar results were obtained for NCEP.

From/To	CT 1+	CT 1-	CT 2+	CT 2-	CT 3+	CT 3-	CT 4+	CT 4-
CT 1+	-	0.0	12.6	33.8	11.3	7.6	8.1	26.6
CT 1-	0.6	-	16.8	14.0	20.7	20.7	22.9	4.5
CT 2+	12.6	15.0	-	0.0	34.5	9.7	9.7	17.5
CT 2-	23.7	15.0	0.4	-	12.9	12.9	19.4	16.4
CT 3+	17.2	14.2	17.7	18.9	-	0.0	16.8	15.1
CT 3-	16.9	12.0	19.7	16.2	0.0	-	10.6	15.1
CT 4+	22.2	16.1	18.9	18.3	18.9	10.5	-	0.0
CT 4-	17.1	20.4	20.8	14.7	17.1	9.0	0.9	-

Table 4: Transition matrix from a circulation type (rows) to a different circulation type (columns) for the ERA-40 classification. The transitions are shown as the proportion of changes from a given circulation type to another one with respect to the total number of changes from the first circulation type.

## 5. Circulation types and modes of variability

CTs and modes of variability are two different approaches to describe the variability of the atmospheric extra-tropical circulation. To estimate the modes of variability, an S-mode PCA of the daily fields has been carried out followed by a varimax rotation. Figure 2b shows the LEV diagram used to determine the number of retained PCs. As in Figure 2a, the four leading PCs show a separation from the remaining PCs and, hence, have been considered for rotation. The rotated eigenvectors can be identified as the following modes of variability: the North Atlantic Oscillation (NAO, with 16.8% of explained variance), the East-Atlantic pattern (EAT, 16.7%), the Scandinavian pattern (SCAN, 15.0%) and the East-Atlantic/Russian (EAWR,

13.7%). These modes have been detected in previous studies (e.g., Barnston and Livezey, 1987). Note that the explained variances are slightly lower than those obtained with weekly or monthly-mean data. However, the patterns and interannual evolution of the modes of variability estimated with daily data are basically the same as those obtained using monthly-mean data (not shown). The time series (the PCs) represent the intensity of the modes of variability for each day.

The PCs have been used to understand the relationship between the classification described in previous sections and the four modes of variability. As daily time series are available for both CTs and modes of variability, the PCs of the modes of variability have been subsampled by extracting the time series corresponding to the days classified in each CT. Figure 7 shows the probability distribution functions (PDFs) for each subsample and the climatological PDF of each mode of variability. The PDFs have been estimated using a Gaussian kernel estimator (Silverman, 1986) with a smoothing parameter of 0.4. Important shifts in the central moment and changes in the kurtosis of the distributions of the subsamples (the central moment for the climatological PDFs is close to zero) can be observed. Concentrating on the NAO mode, a clear separation between CTs associated to either positive or negative NAO can be evidenced. CT1+ seems to be the most clearly associated to the positive NAO (as suggested in previous sections), while CT1- and CT3- show the largest shift to negative NAO values, which suggests that only blocking over the North Atlantic is clearly linked to the negative phase of the NAO, while European blocking (CT2+ and CT4+) gives only moderately negative NAO values. While positive values of the SCAN mode are linked to western European blocking types (CT2+ and CT3+), the negative phase is favoured by ridges over the East Atlantic (CT2- and CT3-). In other words, the SCAN mode is associated with a strong meridional circulation in both of its phases. The CTs are divided in two groups in their relationship to the EAT mode. CT1+, CT2+, CT3- and CT4- shift the EAT PDF towards positive values and CT1-, CT2-, CT3+ and CT4+ towards negative values. The main spatial difference between the two groups of CTs consists in the location of the main meridional features, which are over Europe for the first group and over the Atlantic for the second. Finally, the EAWR mode shows also a separation in two groups, although with different CTs with respect to those involved in the EAT mode. The CTs with the largest differences for this mode are CT4+, which shifts towards positive values, and CT4- towards negative ones. This suggests that the two extreme phases of the EAWR are related to blocked and zonal flows over Europe.

The differences between the PDF of a mode of variability and the one obtained with the sample associated with a particular CT have been assessed with the non-parametric two-sample Kolmogorov-Smirnov test in terms of the so-called Smirnov distance  $D_s$  (Wilks, 2006).  $D_s$  is defined as the maximum absolute difference between two accumulated distribution functions.  $D_s$  is significant at the 5% level for all the subsample distributions of the modes of variability suggesting that the each CT subsamples significantly different parts of the PDF of a given mode of variability. The results agree well with the description shown above. In particular, the SCAN mode discriminates mostly the Euro-Atlantic (CT4+) and the Scandinavian blocking (CT2+); EAWR discriminates the blocked (CT4+) and zonal flows (CT4-) over the North Atlantic; the NAO discriminates the CT most similar to its positive (CT1+) and negative (CT3-) phases, as well as the Atlantic ridge with axis south of Iceland (CT1-); finally, the EAT discriminates especially the Atlantic ridge as an extension of the Azores anticyclone (CT2-). These results indicate that the eight CTs identified here have a distinct influence in the variability of the Euro-Atlantic circulation. Furthermore, this allows the interpretation of monthly or seasonal extreme values of the modes of variability as anomalous successions of CTs, which can follow preferred paths of transitions as described in Section 4.3.

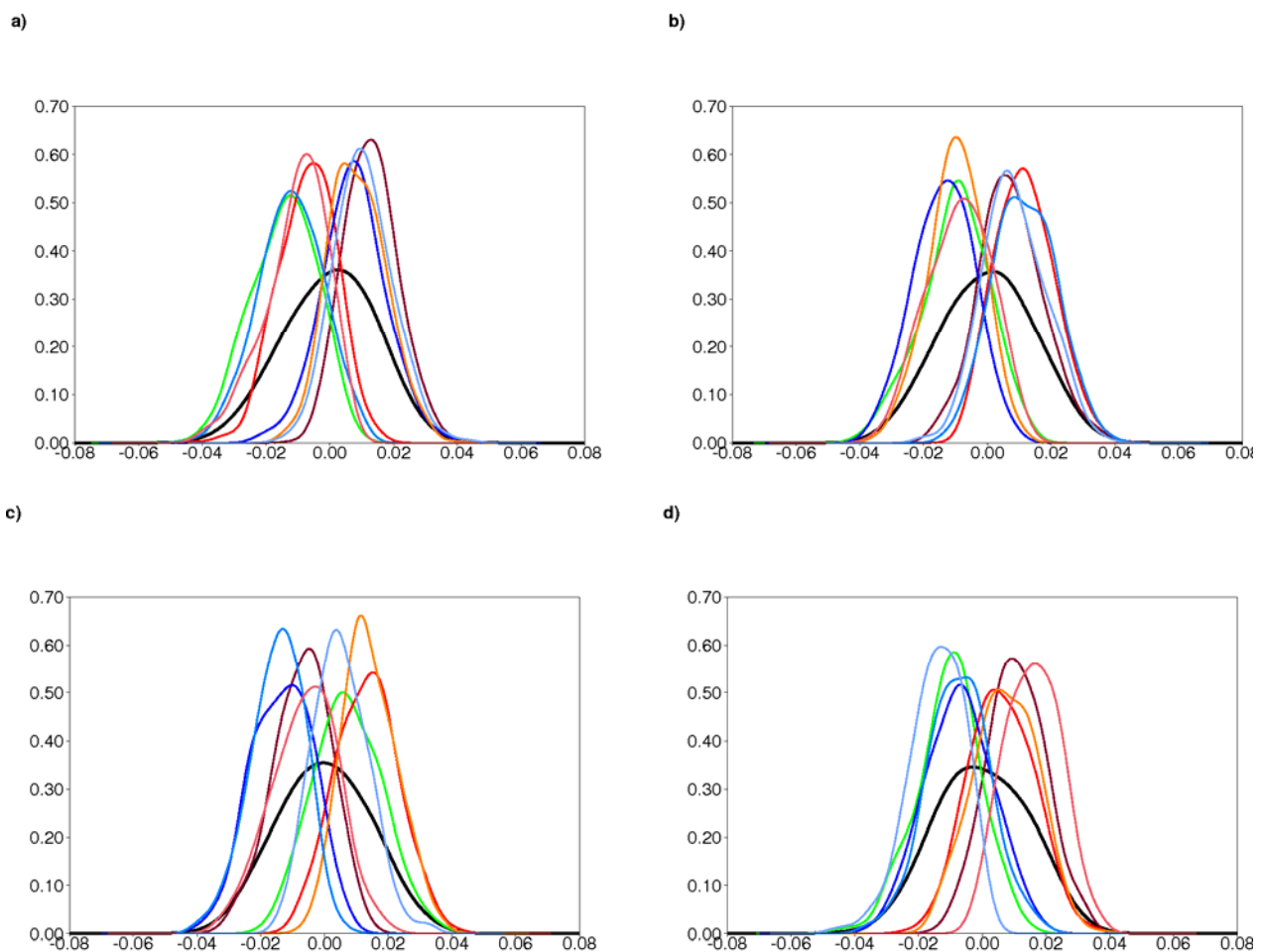


Figure 7: Probability density function (pdf) of the four modes of variability (solid black): a) NAO, b) East Atlantic, c) Scandinavian pattern and d) East-Atlantic/West Russia. For each mode of variability, the pdfs for the days classified in each one of the eight circulation types in the ERA-40 classification over the period 1962-2002 are superposed: CT1+ (burgundy), CT1- (green), CT2+ (red), CT2- (dark blue), CT3+ (orange), CT3- (blue), CT4+ (pink) and CT4- (light blue).

## 6. Circulation types and modes of variability

An objective classification of the Euro-Atlantic atmospheric circulation has been carried out using data from the ERA-40 and NCEP re-analyses. The classification is based on a T-mode PCA followed by a varimax rotation of the four leading PCs. This classification shows most of the features already presented in previous studies. The relative frequencies of the CTs show that the most frequent is a ridge with axis from the Iberian Peninsula to Scandinavia (CT1+), which closely resembles the positive phase of the NAO. The less frequent types are found for ridges over the Atlantic at different latitudes (CTs 3- and 3+). They are also the CTs with the longest (CT3-) and shortest (CT3+) mean duration. The CTs related to blocking events, like CT2+ and CT4+, exhibit higher frequencies in the early 1990s, while a positive trend in the frequency of ridge types is apparent, especially for CT2-. These types increase in frequency from the late 1980s to 2001. Most of the characteristics of the classification are insensitive to the database considered, except for the number of events as a function of their duration, which should be considered as an indication of the lack of robustness of some of the features found in weather classifications with a single dataset. Preferred paths for transition between

specific CTs have been found, an interesting feature to explain low-frequency anomalies in specific seasons and to use as validation tool of weather forecasts and climate simulations.

The main modes of variability for the Euro-Atlantic region (NAO, EAT, SCAN and EAWR) have been estimated using an S-mode PCA on daily data to assess their relationship with the CTs. The CTs show a distinct, statistically significant relation with each mode of variability, as inferred from the subsampled PDFs compared to the PDF obtained for the mode of variability. The probability of finding specific phases of some modes of variability is enhanced for some CTs (for instance, positive phase of NAO with CT1+ or the negative phase with CT3-). The discrimination of the modes of variability by the CTs allows the interpretation of monthly or seasonal extreme values of the modes of variability as anomalous successions of CTs, which can follow preferred paths of transitions. This opens a new way to interpret model errors in climate variability on the basis of the features of a weather classification of these simulations. These later results deserve a more detailed study due to their possible implications for the analysis of climate variability and its simulation in the Euro-Atlantic region.

## 7. Acknowledgements

The authors acknowledge the scientists involved in producing the ERA-40 and NCEP re-analyses. We would like to thank the two anonymous reviewers whose comments significantly contributed to improve the paper. FJDR was supported by the EU-funded ENSEMBLES project (GOCE-CT-2003-505539).

## 8. References

- Barnston AG, Livezey RE (1987) Classification, seasonality, and persistence of low-frequency atmospheric circulation patterns. *Mon Wea Rev* **115**: 1083-1126
- Bartzokas A, Metaxas DA (1996) Northern Hemisphere gross circulation types. Climatic change and temperature distribution. *Meteorologische Zeitschrift* **NF 5**: 99-109
- Blackmon ML, Lee YH, Wallace JM (1984) Horizontal structure of 500 mb height fluctuations with long, intermediate, and short time scales. *J Atmos Sci* **41**: 961-979
- Cheng X, Dunkerton TJ (1995) Orthogonal Rotation of spatial patterns derived from Singular Value Decomposition Analysis. *J Climate* **8**: 2631-2643
- Compagnucci RH, Salles MA (1997) Surface pressure patterns during the year over Southern South America. *Int J Climatol* **17**: 635-653
- Doblas-Reyes FJ, Casado MJ, Pastor MA (2002) Seasonal evolution of Northern Hemisphere blocking frequency to the detection index. *J Geophys Res* **107**, D2 10.1029/2000JD290L07202
- Hess P, Brezowski H (1952) Katalog der Grosswetterlagen Europas. *Berichte des Deutschen Wetterdienstes in der US-Zone*, 33
- Hsu HH, Wallace JM (1985) Vertical structure of wintertime teleconnection patterns. *J Atmos Sci* **42**: 1693-1710

- Huth R (1996) An intercomparison of computer-assisted circulation classification methods. *Int J Climatol* **16**: 893-922
- Huth R (1997) Continental-Scale circulation in the UKHI GCM. *J Climate* **10**: 1545-1561
- Huth R (2000) A circulation classification scheme applicable in GCMs studies. *Theor Appl Climatol* **67**: 1-18
- James P (2007) An objective classification method for Hess and Brezowsky Grosswetterlagen over Europe. *Theor Appl Climatol* **88**: 17-42
- Jiang N, Hay JE, Fisher GW (2006) Classification of New Zealand Synoptic Weather Types and Relation to the Southern Oscillation Index. *Weather and Climate* **25**: 43-70
- Kalnay E et al. (1996) The NCEP/NCAR 40 year re-analysis project. *Bull Amer Meteor Soc* **77**: 437-471
- Key J, Crane RG (1986) A comparison of synoptic classification schemes based on objective procedures. *J Climatol* **6**: 375-388
- Kidson JW (1994) An automated procedure for the identification of synoptic types applied to the New Zealand region. *Int J Climatol* **14**: 711-721
- Kirchhofer W (1973) Classification of European 500 mb patterns. *Arbeitsbericht der Schweizerischen Meteorologischen Zentralanstalt* 43
- Kyselý J, Huth R (2006) Changes in atmospheric circulation over Europe detected by objective and subjective methods. *Theor Appl Climatol* **85**: 19-36
- Kyselý J, Domonkos P (2006) Recent increase in persistence of atmospheric circulation over Europe. Comparison with long term variations since 1881. *Int J Climatol* **26**: 461-483
- Lamb HH (1950) Types and spells of weather around the year in the British Isles: annual trends, seasonal structure of the year singularities. *Quart J Roy Meteor Soc* **76**: 393-429.
- Lund IA (1963) Map-pattern classification by statistical methods. *J Appl Meteorol* **2**: 56-65
- Michelangeli PA, Vautard R, Legras B (1995) Weather regimes: Recurrence and quasi stationarity. *J Atmos Sci* **52**: 1237-1256
- Plaut G, Simonnet E (2001) Large-scale circulation classification, weather regimes, and local climate over France, the Alps and Western Europe. *Clim Res* **17**: 303-324
- Richman MB (1986) Rotation of principal components. *J Climate* **6**: 293-335
- Richman MB (1999) Relationships between the definition of the hyperplane width to the fidelity of Principal Component Loading Patterns. *J Climate* **12**: 1557-1576.

SánchezGómez E, Terray L (2005) Large-scale atmospheric dynamics and local intense precipitation episodes. *Geophys Res Lett* **32**:L24711, doi:10.1029/2005GL023990

Silverman BW (1986) *Density Estimation*. Chapman and Hall, London, 175 pp

Slonosky VC, Jones PD, Davies TD (2000) Variability of the surface atmospheric circulation over Europe, 1774-1995. *Int J Climatol* **20**: 1875-1897

Thompson DWJ, Wallace JM (1998) The Arctic Oscillation signature in the wintertime geopotential height and temperature fields. *Geophys Res Lett* **25**: 1297-1300

Uppala SM, Kållberg PW, Simmons AJ, Andrae U, da Costa Bechtold V, Fiorino M, Gibson JK, Haseler J, Hernandez A, Kelly GA, Li X, Onogi K, Saarinen S, Sokka, N, Allan RP, Andersson E, Arpe K, Balmaseda MA, Beljaars ACM, van de Berg L, Bidlot J, Bormann, N, Caires S, Chevallier F, Dethof A, Dragosavac M, Fisher M, Fuentes M, Hagemann S, Hólm E, Hoskins BJ, Isaksen L, Janssen PAEM, Jenne R, McNally AP, Mahfouf JF, Morcrette JJ, Rayner NA, Saunders RW, Simon P, Sterl, A, Trenberth KE, Untch A, Vasiljevic D, Viterbo P, and Woollen J (2005) The ERA-40 re-analysis. *Quart J Roy Meteor Soc* **131**: 2961-3012.doi:10.1256/qj.04.176

Von Storch H, Zwiers FW (1999) *Statistical Analysis in Climate research*. Cambridge University Press, 510 pp

Werner PC, Gerstengarbe FW, Fraedrich K, Oesterle H (2000) Recent climate change in the North Atlantic European sector. *Int J Climatol* **20**: 463-471

Wilks DS (2006) *Statistical Methods in the Atmospheric Science*. Academic Press, 627 pp

Yiou P, Nogaj M (2004) Extreme climatic events and weather regimes over the North Atlantic: When and where?. *Geophys Res Lett* **31**: L07202, doi: 10.1029/2003GL019119